

Involvement of glutathione peroxidase 1 in growth and peroxisome formation in *Saccharomyces cerevisiae* in oleic acid medium

Takumi Ohdate^{a, b}, and Yoshiharu Inoue^{a, *}

Running title: Yeast Gpx1 is involved in peroxisome biogenesis

^aLaboratory of Molecular Microbiology, Division of Applied Life Sciences, Graduate School of Agriculture, Kyoto University, Japan

^bDepartment of Microbiology, Tohoku Pharmaceutical University, Japan

* Corresponding author at: Laboratory of Molecular Microbiology, Division of Applied Life Sciences, Graduate School of Agriculture, Kyoto University, Uji, Kyoto 611-0011, Japan. Tel.: +81 774-38-3773; fax.: +81 774-38-3789.

E-mail address: y_inoue@kais.kyoto-u.ac.jp (Y. Inoue).

Abbreviations: ROS, reactive oxygen species; GPx, glutathione peroxidase; PTS, peroxisome targeting signal; ER, endoplasmic reticulum; SD, synthetic dextrose; PMSF, phenylmethylsulfonyl fluoride; PAGE, polyacrylamide gel electrophoresis; 3-AT, 3-amino 1,2,4-triazole; *t*-BHP, *tert*-butyl hydroperoxide.

Highlights

S. cerevisiae has three glutathione peroxidase homologues. The expression of Gpx1 was induced when cells were cultured in oleic acid medium. Gpx1 was present in the peroxisomal matrix. Deficiency in Gpx1 impaired growth and peroxisome formation in oleic acid medium. Redox regulation of Gpx1 is involved in peroxisome biogenesis.

Abstract

Saccharomyces cerevisiae is able to use some fatty acids, such as oleic acid, as a sole source of carbon. β -Oxidation, which occurs in a single membrane-enveloped organelle or peroxisome, is responsible for the assimilation of fatty acids. In *S. cerevisiae*, β -oxidation occurs only in peroxisomes, and H_2O_2 is generated during this fatty acid-metabolizing pathway. *S. cerevisiae* has three *GPX* genes (*GPX1*, *GPX2*, and *GPX3*) encoding atypical 2-Cys peroxiredoxins. Here we show that expression of *GPX1* was induced in medium containing oleic acid as a carbon source in an Msn2/Msn4-dependent manner. We found that Gpx1 was located in the peroxisomal matrix. The peroxisomal Gpx1 showed peroxidase activity using thioredoxin or glutathione as a reducing power. Peroxisome biogenesis was induced when cells were cultured with oleic acid. Peroxisome biogenesis was impaired in *gpx1* Δ cells, and subsequently, the growth of *gpx1* Δ cells was lowered in oleic acid-containing medium. Gpx1 contains six cysteine residues. Of the cysteine-substituted mutants of Gpx1, Gpx1^{C36S} was not able to restore growth and peroxisome formation in oleic acid-containing medium, therefore, redox regulation of Gpx1 seems to be involved in the mechanism of peroxisome formation.

Keywords: glutathione peroxidase, peroxisomes, yeast, peroxiredoxin, reactive oxygen species

1. Introduction

Lipids are one of the energy storage forms in cells. Fatty acids are constituents of lipids, from which an enormous amount of energy can be drawn. The process to draw energy from fatty acids is referred to as β -oxidation. In mammalian cells, β -oxidation occurs in mitochondria and peroxisomes [1]. In the first step of β -oxidation, fatty acyl-CoA is generated from fatty acid, ATP, and CoA by an action of acyl-CoA synthetase in the cytoplasm, and is transported to the mitochondrial matrix with the aid of carnitine. After which, fatty acyl-CoA is oxidized to *trans*- Δ^2 -enoyl-CoA by acyl-CoA dehydrogenase. In this reaction, FAD is used as an acceptor of an electron from acyl-CoA, and the FADH₂ formed enters the electron transfer chain in mitochondria to produce ATP. The mitochondrial β -oxidation is responsible for moderately long chain fatty acids ($\sim C_{18}$); whereas, the β -oxidation in peroxisomes is responsible for very long chain fatty acids ($>C_{20}$) [1]. The budding yeast *Saccharomyces cerevisiae* is also able to use fatty acids as a sole source of carbon. Unlike mammalian cells, *S. cerevisiae* shows β -oxidation only in peroxisomes, the biogenesis of which is markedly induced when yeast cells

are cultured in a medium containing fatty acids. The first step of β -oxidation in the yeast peroxisome is carried out by acyl-CoA oxidase. In this enzymatic reaction, molecular oxygen (O_2) is used as the final acceptor of electrons from acyl-CoA, and consequently, H_2O_2 is generated in the peroxisome. In the final step of β -oxidation, 3-ketoacyl-CoA thiolase liberates acetyl-CoA which results in 3-ketoacyl-CoA esters being converted into a C_2 -shortened acyl-CoA. Acetyl-CoA generated from the β -oxidation of fatty acids is entered into the glyoxylate cycle. Enzymes constituting the glyoxylate cycle are located on both sides of peroxisomal membrane [2]. Succinate is released from the glyoxalate cycle, and transported into mitochondria. Alternatively, acetyl-CoA is transported from peroxisomes to mitochondria in a carnitine-dependent manner. Recent studies have revealed that there are several options for transferring acyl groups from peroxisomes to mitochondria [for review, see Ref. 3]. Consequently, ATP is produced in mitochondria [4]. In this way, the process to draw energy from fatty acids is aerobic, and so has the potential to produce a large amount of reactive oxygen species (ROS). Indeed, H_2O_2 is generated in the first step of β -oxidation in yeast, and the respiration process in mitochondria is also capable of generating ROS. To reduce the risk of oxidative stress caused by ROS during the metabolism of fatty acids, *S. cerevisiae* has a peroxisomal catalase, encoded by *CTA1*, whose expression is induced in medium containing fatty acids [5].

Besides catalase, *S. cerevisiae* has several antioxidative enzymes that are able to scavenge H_2O_2 . Peroxiredoxins are a growing family of antioxidants in many eukaryotic organisms. Since peroxiredoxins do not contain a redox active cofactor or prosthetic group, the redox status of cysteine residues plays crucial roles in peroxidase reactions [6]. Peroxiredoxins are classified into three groups depending on the number of conserved cysteine residues, i.e. 1-Cys, 2-Cys, and atypical 2-Cys peroxiredoxins [7]. *S. cerevisiae* has one 1-Cys peroxiredoxin (Prx1), and four 2-Cys peroxiredoxins (Tsa1, Tsa2, Ahp1, and Dot5) [8]. We have previously reported that *S. cerevisiae* has three glutathione peroxidases (Gpx1, Gpx2, and Gpx3), which are structural homologues of the mammalian glutathione peroxidase (GPx) [9]. After biochemical characterizations, these GPx homologues have been revealed to be atypical 2-Cys peroxiredoxins [10-12]. These peroxiredoxins use thioredoxin, a protein-disulfide oxidoreductase, as a reducing power to revert the critical oxidized cysteine(s) to retain the integrity of enzymatic activity. Gpx1 and Gpx2 are able to use glutathione also. Among yeast peroxiredoxins, Prx1 is distributed in mitochondria, Dot5 in the nucleus, Ahp1 in mitochondria and/or peroxisomes, and Tsa1/2 in the cytoplasm [8]. The intracellular distribution of GPx

homologues has not yet been elucidated, except for Gpx2, which we have recently identified to be located in mitochondria [13]. In this study, we found that *GPX1* expression is induced by oleic acid, and a *gpx1Δ* mutant showed slow-growth phenotype in oleic acid-containing medium. We showed that Gpx1 is located in the peroxisomal matrix, and the peroxisomal Gpx1 exhibits peroxidase activity. Finally, we investigated the correlation between Gpx1 and peroxisome biogenesis.

2. Material and methods

2.1. Strains

All *S. cerevisiae* strains used in this study have the BY4741 background. The strains and PCR primers used are summarized in Supplementary Tables S1 and S2, respectively.

The *gpx1Δ::his5⁺* mutant was generated by replacing *kanMX4* of *gpx1Δ::kanMX4* mutant in the BY4741 background with a *his5⁺* cassette in pUG27. When combining other mutations constructed by the *kanMX4* marker with deletion of *gpx1Δ::his5⁺* fragment was amplifying with primers, GPX1-F and GPX1-R, and the resultant fragment was introduced to the mutant strains with the *kanMX4* marker. To construct *gpx3Δ::LEU2* and *msn2Δ::HIS3* mutants in the BY4741 background, each mutation allele in the YPH250-based mutant was amplified using primer sets as described before [9, 14]. To construct a strain carrying GFP-tagged Vps1, PCR was done using primers VPS1-GFP-F and VPS1-GFP-R with the genomic DNA of VPS1-GFP (BY4742 background) [15] as a template. The resultant PCR fragment containing the C terminus half of Vps1 tagged with GFP and nourseothricin-resistant gene was introduced into the *VPS1* locus, and clones showing the resistance to nourseothricin were isolated.

2.2. Plasmids

The plasmids constructed in this study are summarized in Supplementary Table S3.

To construct pRS416+GPX1-3HA, pSLF172-GPX1 [16] was digested with Sall and HindIII, and the *GPX1-3HA* cassette was inserted into the Sall-HindIII site of pRS416. To construct pRS306+GPX1-3HA, PCR was done using primers GPX1-F-XbaI and GPX1-R-BamHI with pSFL172-GPX1 as a template, and the XbaI/BamHI fragment was inserted into the XbaI-BamHI site of pRS306. pRS306+GPX1-3HA was digested with EcoRI, and integrated into the *GPX1* locus of BY4741. To construct pRS414-GPX1, the *GPX1* gene was amplified using GPX1-Sall-F and GPX1-PstI-R. Sall and PstI site were designed in

GPX1-Sall-F and GPX1-PstI-R, respectively (underlined). The PCR fragment was digested with Sall and PstI, and the resultant fragment was cloned into the Sall and PstI site of pRS414. To construct pRS411+GPX1, pRS416+GPX1 and pRS426+GPX1, pRS414+GPX1 as constructed above was digested with Sall and BamHI, and the DNA fragment containing *GPXI* was cloned into the Sall-BamHI site of pRS411, pRS416, and pRS426, respectively.

To construct pRS416+GPX2, pRS416+GPX3, pRS411+GPX2, and pRS411+GPX3, the *GPX2* and *GPX3* gene was amplified using GPX2-Sall-F and GPX2-BamHI-R, or GPX3-Sall-F and GPX3-BamHI-R using genomic DNA of BY4741 as a template. Sall and BamHI site were designed in each forward primer (F), and reverse primer (R), respectively (underlined). Each PCR fragment was digested with Sall and BamI, and the resultant fragment was cloned into the Sall and BamI site of pRS416 or pRS411.

To construct pRS411-based Gpx1-3HA cysteine-to-serine variants, pRS416-based Gpx1-3HA cysteine-to-serine variants [12] were digested with Sall and XbaI, and each DNA fragment containing *GPXI* was cloned into the XhoI-SpeI site of pRS411.

To construct *POT1-GFP* plasmid, the first PCR was done using POT1-F and POT1-R using the genomic DNA of BY4741 as a template. SacI and BamHI site were designed in POT1-F and POT1-R, respectively (underlined). The PCR fragment was digested with SacI and BamHI, and the DNA fragment containing a part of *POT1* was cloned into the SacI-BamHI site of pKW430 [17]. The resultant plasmid was digested with SacI and XhoI, and the resultant fragment containing *POT1-GFP* was cloned in to the SacI-XhoI site of pRS306. pRS306+POT1-GFP was digested with EcoRI, and integrated into the *POT1* locus of BY4741.

To construct *HA-POXI* plasmid, the first PCR was done with the following primer sets: POX1-F-Sall plus POX1-HA-R, and POX1-HA-F plus POX1-R+900 using the genomic DNA of BY4741 as a template. Sall site was designed in POX1-F-Sall (underlined). The second PCR was done using the primers POX1-F-Sall and POX1-R+900, with the mixture of the first PCR products as a template. The second PCR products were digested with Sall and BamHI, and the DNA fragment containing *HA-POXI* was cloned into the Sall-BamHI site of pRS306. pRS306+HA-POX1 was digested with HindIII, and integrated into the *POXI* locus of BY4741. To construct pRS421+POX1, the *POXI* gene was amplified using POX1-F-Sall and POX1-R-EagI. Sall and EagI sites were designed in POX1-F-Sall and POX1-R-EagI, respectively (underlined). The PCR fragment was digested with Sall and EagI, and the resultant fragment was cloned into the Sall-EagI site of pRS421.

2.3. Growth experiment

The media used were synthetic dextrose (SD) medium (2% glucose and 0.67% yeast nitrogen base without amino acids) with appropriate amino acids, YPOT medium (1% yeast extract, 2% peptone, 0.2% oleic acid, and 0.2% Tween 40), and YNBOT medium [0.67% yeast nitrogen base (without amino acids) with appropriate amino acids and bases, 0.15% oleic acid, and 0.15% Tween 40].

To monitor the growth of cells in oleic acid-containing medium, cells grown in SD medium until $A_{610}=1.0$ were collected by centrifugation, washed once with a 0.85% NaCl solution, and suspended in YNBOT medium. Since oleic acid is difficult to dissolve in water, a detergent (Tween 40) was added to the medium. However, the A_{610} varied among experiments even though Tween 40 was added and the same yeast strain was used, which may be due to the difference in solubility of oleic acid in the medium in each experiment. To minimize the dispersion of the data, cell growth was expressed relative to the final A_{610} of the wild type in each experiment after a 216-h culture in YNBOT medium. The relative growth was expressed as the rate of A_{610} of each strain at each time versus A_{610} of wild type after 216-h culture, calculated with the following equation: $[(A_{610} \text{ of each strain at each culture time} - 1.0)/(A_{610} \text{ of wild type at 216-h culture} - 1.0)] \times 100$.

2.4. Western blotting

Cells cultured in YPOT or YNBOT medium were disrupted with glass beads in 10 mM Tris-HCl buffer (pH 7.0) containing 1 mM phenylmethylsulfonyl fluoride (PMSF). Homogenates were centrifuged at 2000 x g for 10 min at 4°C. The supernatants were subjected to reducing SDS-polyacrylamide gel electrophoresis (PAGE), and the separated proteins were transferred to a PVDF membrane (Millipore).

The expression of Pot1, Cta1, Gpx3, Pex11, and Ahp1 was determined using anti-Pot1 [18], anti-Cta1 [19], anti-Gpx3 [20], anti-Pex11 [21], and anti-Ahp1 [22] antibodies, respectively. The expression of HA-tagged Gpx1 or Dnm1 (pRS426+Dnm1-HA) [23] and GFP-tagged Vps1 was determined using anti-HA monoclonal antibody (Cell Signaling) and anti-GFP monoclonal antibody (Santa Cruz Biotechnology), respectively.

2.5. Anti-Gpx1 antibodies

The purified recombinant Gpx1 expressed in *E. coli* [12] was used to immunize New Zealand White rabbits to raise anti-Gpx1 antibodies. The validity of anti-Gpx1 antibodies was

determined by Western blotting using different *gpxΔ* mutants. As shown in Supplementary Fig. S1, the antibodies raised crossed with not only Gpx1 but also Gpx3.

2.6. Subcellular fractionation and isolation of peroxisomes

Organelle pellet (P20) and post nuclear supernatant (cytosolic fraction) (S20) were prepared as described by Smith et al. [24]. P20 was suspended in chilled gradient buffer [5 mM MES (pH 5.6), 0.65 M sorbitol, 1 mM KCl, 1 mM EDTA, 1 mM PMSF, and protease inhibitor (Nakalai tesque)], and the suspension (1 mg protein) was overlaid onto a step-wise gradient of Nycodenz in MS buffer [5 mM MES (pH 5.6), 0.65 M sorbitol, 1 mM KCl, 1mM EDTA, and 1 mM PMSF]. The Nycodenz gradient was as follows (from the bottom of the tube): 0.5 ml 50% Nycodenz, 2.5 ml 35%, 2.5 ml 23%, and 2.5 ml 10% (total volume, 8 ml). Organelles were separated by ultracentrifugation at 130000 x *g* for 2.5 h at 2°C with Himac CP75b (Hitachi Koki). Each fraction was collected 0.65 ml from the top of the tube, and the distribution of proteins of interest was analyzed by Western blotting. Anti-Pgk1 antibodies (Cell Signaling) were used to detect Pgk1 as a cytoplasmic marker. The localization of thioredoxin and Glr1 was determined using Anti-Trx2 antibodies [25] and anti-Glr1 antibodies [26], respectively. Anti-Trx2 antibodies cross react with Trx1 [25].

2.7. Fractionation of peroxisomes

Peroxisomes were fractionated as described by Fujiki et al. [27] but with some modifications. The peroxisomal fraction, purified by Nycodenz gradient ultracentrifugation, was suspended in 10 mM Tris-HCl buffer (pH 8) containing 1 mM PMSF, and kept on ice for 2 h. By hypoosmotic shock, peroxisome is ruptured, and matrix proteins are released. The suspension was centrifuged at 200000 x *g* for 1 h at 4°C in Himac CS120 (Hitachi Koki). The pellet was suspended in salt extraction buffer [10 mM Tris-HCl (pH 8), 1 M NaCl, and 1 mM PMSF] on ice for 1 h, and centrifuged at 200000 x *g* for 1 h at 4°C. The pellet was suspended in high pH extraction buffer [10 mM Tris-HCl (pH 8), 100 mM Na₂CO₃, and 1 mM PMSF], kept on ice for 1 h, and centrifuged at 200000 x *g* for 1 h at 4°C. TCA (20%) was added to the supernatant to precipitate protein. The suspension was centrifuged at 15100 x *g* for 10 min at 4°C, and the pellet was washed with acetone. Equal amounts of protein in each fraction were separated by SDS-PAGE followed by Western blotting. Anti-Pcs60 [28] and anti-Pex13 [29] antibodies were used to detect Pcs60 (membrane-associated protein) and Pex13 (membrane-integral protein), respectively.

2.8. Proteinase K assay

The proteinase K assay was performed as described by Höhfeld et al. [30] but with some modifications. The peroxisomal fraction, purified by Nycodenz gradient ultracentrifugation without PMSF, was divided into two portions (each portion: 1 ml). One portion was treated with 0.1% Triton X-100 at room temperature for 30 min, followed by 10 µg/ml proteinase K (Nacalai tesque) at room temperature. The other portion was treated with proteinase K without pretreatment with Triton X-100 after 30 min at room temperature. After 0, 5, 10, 20, 40, 60, 90, and 120 min, an aliquot (100 µl) of each sample was mixed with TCA (final concentration, 20%). The suspension was centrifuged at 15100 x g for 10 min at 4°C, and the pellet was washed with acetone. Equal amounts of the protein fraction were separated by SDS-PAGE followed by Western blotting.

2.9. Fractionation of mitochondria

Mitochondria were fractionated as described by Yamamoto et al. [31]. The mitochondrial fraction, purified by Nycodenz gradient ultracentrifugation, was treated with salt extraction buffer [0.6 M sorbitol, 10 mM Tris-HCl (pH7.4), 500 mM NaCl] or high pH extraction buffer [0.6 M sorbitol, 10 mM Tris-HCl (pH7.4), 100 mM Na₂CO₃] for 1 h on ice, and centrifuged at 200000 x g for 1 h at 4°C. TCA (20%) was added to the supernatant to precipitate protein. Each suspension was centrifuged at 15100 x g for 10 min at 4°C, and the pellet was washed with acetone. Equal amounts of protein in each fraction were separated by SDS-PAGE followed by Western blotting. Anti-Por1 antibodies (Cell Signaling) and anti-Hsp60 antibodies [32] were used to detect Por1 (mitochondrial outer membrane marker protein) and Hsp60 (mitochondrial matrix marker protein), respectively.

2.10. Preparation of peroxisomal matrix protein

Cells were cultured in YNBOT medium for 20 h, and 50 mM 3-amino 1,2,4-triazole (3-AT) was added. Cells were incubated for 5 h to inhibit catalase [33]. Peroxisomes were purified by Nycodenz gradient ultracentrifugation as described above. For preparation of peroxisomal matrix protein, the purified peroxisomes were disrupted with a sonicator. The membrane fraction was removed by centrifugation at 200000 x g for 1 h at 4°C, and 10 mM 3-AT was added to the supernatant. After being incubated at 4°C for 5 h, the supernatant was used as the source of enzyme.

2.11. Microscopy

Cells carrying DsRed-PTS1 [24] or Pot1-GFP were grown in SD medium until $A_{610}=1$, and transferred to YNBOT medium. Cells were collected at prescribed times, washed once with a 0.85% NaCl solution, and suspended in the same solution. Distributions of DsRed-PTS1 or Pot1-GFP were observed using fluorescence microscopy. The localization of Gpx1-3HA in *gpx1* Δ cells was examined by indirect immunofluorescence microscopy using anti-HA monoclonal antibody. The cells were stained for DNA with 1 μ g/ml 4',6'-diamino-2-phenylindole dihydrochloride (DAPI).

3. Results and discussion

3.1. Expression of *Gpx1* was induced by oleic acid

Since H₂O₂ is unavoidably generated during β -oxidation in yeast peroxisomes, it is conceivable that the expression of antioxidative enzymes is linked with fatty acid metabolism. Previously, we have reported that the expression of *GPX1* was induced when cells were cultured in a medium containing non-fermentable carbon, such as glycerol [16]. Fatty acids are also a source of non-fermentable carbon for yeast cells, so we investigated the role of Gpx1 in the assimilation of fatty acids. To determine whether the expression of *GPXs* is induced when cells are cultured in medium containing oleic acid, we monitored the protein levels of each GPx homologue. As we have reported previously, Gpx1 protein was not detected in cells at the log phase of growth in glucose medium (Fig. 1A, time 0 h) [16]. However, upon the shift to YPOT medium, Gpx1 protein began to be detected (~3 h), and the level of Gpx1 protein peaked after 24-36 h (Fig. 1A). On the other hand, the expression of Gpx2 and Gpx3 was not induced by oleic acid, i. e. the levels of these proteins were kept constant throughout the growth phase (Fig. 1A). We monitored the expression of Pot1 (thiolase) and Cta1 (catalase) in YPOT medium. Both Pot1 and Cta1 are present in the peroxisomal matrix, and the expression of genes encoding these proteins is induced by oleic acid [5]. Timing of the expression of *GPX1*, *POT1*, and *CTA1* was consistent with each other (Fig. 1A).

Previously, we have revealed that Msn2 and Msn4, C₂H₂ zinc-finger transcription factors, play crucial roles in the expression of Gpx1 under glucose-starved conditions [16]. To investigate whether Msn2 and Msn4 are involved in the oleic acid-induced expression of Gpx1, the levels of Gpx1 protein in *msn2* Δ *msn4* Δ cells in YPOT medium were determined. As shown in Fig. 1B, the expression of Gpx1 was greatly reduced in the *msn2* Δ *msn4* Δ mutant. The levels

of Pot1 and Cta1 proteins were slightly reduced in *msn2Δmsn4Δ* cells, although they were still induced in oleic acid medium. These results indicate that Msn2 and Msn4 play important roles in the expression of Gpx1 in oleic acid-containing medium.

3.2. Slow-growth phenotype of *gpx1Δ* cells in oleic acid-containing medium

Since the expression of *GPX1* was markedly induced after transferring glucose-grown cells to oleic acid-containing medium, Gpx1 may have a role in growth in the presence of oleic acid. To address this issue, we monitored the growth of various mutants defective in the *GPX* genes in oleic acid medium. As shown in Fig. 2A, the *gpx1Δ* mutant exhibited approximately 75% growth compared to the wild type in YNBOT medium. Although a deletion of either *GPX2* or *GPX3* did not affect the growth in oleic acid medium, the growth of the *gpx1Δgpx3Δ* mutant was impaired compared with that of the *gpx1Δ* single mutant, and *gpx1Δgpx2Δgpx3Δ* showed an even more severe growth defect. These results suggest that Gpx2 and Gpx3 may have redundant functions with Gpx1 in terms of growth in oleic acid medium. Introduction of *GPX1* with a single copy plasmid restored the growth of the *gpx1Δgpx2Δgpx3Δ* mutant to the level in the *gpx2Δgpx3Δ* mutant (Fig. 2B). Collectively, Gpx1 seems to help yeast cells to grow in oleic acid medium.

It is conceivable that lipid peroxidation may occur during long-term aerobic culture of yeast cells in oleic acid medium. However, since the *gpx1Δ* mutant does not show increased susceptibility to *tert*-butyl hydroperoxide (*t*-BHP) [9], a representative of lipid hydroperoxides, the slow-growth phenotype of *gpx1Δ* cells in oleic acid medium is not likely to be due to lipid hydroperoxides in the medium. However, Gpx1 is an antioxidative enzyme [12], and H₂O₂ is produced during the assimilation of fatty acids in peroxisomes. Indeed, a *CTA1* deletion mutant exhibited 30% growth, possibly due to the loss of peroxisomal catalase activity to scavenge H₂O₂ produced during the assimilation of oleic acid (Fig. 2A). So, the loss of antioxidative activity may influence growth in oleic acid medium. Besides three GPxs, *S. cerevisiae* has five peroxiredoxins (Tsa1, Tsa2, Prx1, Dot5, and Ahp1), and a cytosolic catalase, Ctt1. We monitored the growth of cells lacking these enzymes, however, such mutants did not show any growth defect in oleic acid medium as compared with *gpx1Δ* and *cta1Δ* mutants (data not shown).

3.3. *Gpx1* occurs in peroxisomes

To explore the role of Gpx1 in growth in oleic acid-containing medium, we

determined the localization of Gpx1. We first constructed a GFP-tagged Gpx1. However, since Gpx1-GFP did not complement the slow-growth phenotype of *gpx1* Δ cells in oleic acid-containing medium (data not shown), we adopted the indirect immunofluorescence microscopy using Gpx1-3HA. Since Gpx1-3HA (pRS416+Gpx1-3HA) was able to restore the growth of *gpx1* Δ *gpx2* Δ *gpx3* Δ cells in oleic acid medium as the same extent as Gpx1 without HA-tag (see Fig. 2B), the addition of HA-tag at the C terminus of Gpx1 does not seem to affect the function and localization of Gpx1. Gpx1-3HA was observed as punctate structures in cells grown in oleic acid medium, although the fluorescence signals were not observed in vacuole and the nucleus that is stained with DAPI. Some Gpx1-3HA signals were merged with DAPI signals scattered in cells, which represent mitochondria, but some were not (Supplementary Fig. S2A). Considering that the growth of *gpx1* Δ cells were impaired in oleic acid-containing medium, Gpx1-3HA signals that were not merged with DAPI signals may represent peroxisomes. To further verify the localization of Gpx1, we next adopted the biochemical approach.

Cells grown in oleic acid medium were homogenized, and the cytoplasmic fraction (S20) and mitochondrial/peroxisomal fraction (P20) were separated. Pgk1, a marker of the cytoplasm, was found in the S20 fraction, while Pot1 (peroxisome marker) and Por1 (mitochondria marker) were found in the P20 fraction. As shown in Fig. 3A, Gpx1 was detected in both fractions. Then we tried to separate mitochondria and peroxisomes by Nycodenz gradient ultracentrifugation. Judging from the distribution of marker proteins, the mitochondria and peroxisomes were successfully separated; nonetheless, Gpx1 was found in both (Fig. 3A). So, we concluded that Gpx1 is present in the cytoplasm, peroxisomes, and mitochondria in cells cultured in oleic acid medium.

In this experiment, we used anti-Gpx1 antibodies to determine the distribution of the Gpx1 protein. Since our anti-Gpx1 antibodies cross react with Gpx3 (Supplementary Fig. S1), the band with higher molecular weight in the blots of Gpx1 corresponds to Gpx3, which was confirmed using anti-Gpx3 antibodies (Supplementary Fig. S2B). We verified that anti-Gpx3 antibodies do not cross react with Gpx1 (data not shown). Therefore, we found that Gpx3 is also present in both peroxisomes and mitochondria as well as the cytoplasm when cells are cultured in oleic acid medium. In addition, we found that glutathione reductase and thioredoxin were also located in the peroxisomes (Fig. 3A).

3.4. Mitochondrial localization of Gpx1

Besides peroxisomes, we found that Gpx1 was present in mitochondria also (Fig. 3A). To explore the mode of existence of Gpx1 in mitochondria, we treated purified mitochondria with NaCl or Na₂CO₃ (Fig. 3B). Gpx1 was released from mitochondria to the supernatant fractions after treatment with 500 mM NaCl. Por1 (mitochondrial membrane-integral protein) was not released from mitochondria under the same conditions, and was recovered from the pellets after centrifugation of salt-treated extracts. Hsp60 (mitochondrial matrix protein) was slightly released following treatment with NaCl, but large proportion remained in the pellets. Next, we treated purified mitochondria with 100 mM Na₂CO₃. Since Na₂CO₃ destroys mitochondrial membrane, Hsp60 was released to supernatants. Gpx1 was also detected in the supernatants following treatment with Na₂CO₃. Since Por1 is integrated in the membrane, it was recovered from the residual pellets after centrifugation of high pH-treated mitochondria. Taken together, Gpx1 is a peripheral protein on the outer membrane of mitochondria *via* ionic interaction.

Recently, we found that Gpx2 in cells cultured in glucose medium is located in the cytoplasm and mitochondria [13]. When cells were cultured in oleic acid medium, Gpx2 was scarcely detected in the cytoplasmic fraction, but was found in the mitochondrial/peroxisomal fraction in cells cultured in YPOT medium (Fig. 3A). The Nycodenz gradient ultracentrifugation revealed that Gpx2 is located in mitochondria (Fig. 3A). We verified that anti-Gpx2 antibodies used in this study [11] do not cross react with Gpx1 and Gpx3 (data not shown). Aerobic conditions are rigorously required for yeast cells to assimilate fatty acid as a source of carbon, and subsequently, ROS are generated in both peroxisomes and mitochondria, therefore, it may be reasonable that GPxs are present in these organelles, when cells were cultured in medium containing oleic acid.

3.5. *Gpx1 is present in the peroxisomal matrix*

Next, we determined the localization of Gpx1 in peroxisomes by fractionation (Fig. 3C). The purified peroxisome was suspended in a buffer without sorbitol to rupture peroxisomes. By hypoosmotic shock, peroxisomal matrix proteins are released (Fig. 3C, lane 2). The resulting pellets were suspended in a buffer containing 1 M NaCl followed by ultracentrifugation. By this treatment, proteins that associate with peroxisomal membrane through ionic interaction are released (lane 3). The pellets were further treated with 100 mM Na₂CO₃, and the supernatant (lane 4) and pellets (lane 5) were again separated by ultracentrifugation. Pot1 (matrix protein), Pcs60 (peripheral membrane protein), and Pex13 (membrane integral protein) were detected,

respectively, in the soluble fraction after hypoosmotic shock, the salt-extracted fraction, and the residual pellets after high pH-treatment (Fig. 3C). Since the peroxisomal marker proteins were adequately detected in the respective fractions, we concluded that the fractionation of peroxisomes succeeded. Gpx1 was detected in the same fraction as Pot1 (Fig. 3C, lane 2), therefore, Gpx1 seems localized in the peroxisomal matrix. Additionally, Gpx3 was also found to be localized in the peroxisomal matrix.

We further verified the localization of Gpx1 in the peroxisomal matrix using proteinase K. Thiolase, encoded by *POT1*, is present in the peroxisomal matrix, and consequently, Pot1 was protected from proteinase K in the absence of Triton X-100 (Fig. 3D). When the purified peroxisomes were pretreated with Triton X-100, the molecular weight of Pot1 was shortened by 3 kDa after a 5-min proteinase K treatment, and completely digested after 60 min. By contrast, the intact Pot1 was observed after 120 min of proteinase K-treatment without Triton X-100, although the 3kDa-shortend Pot1 was observed after 40 min. These results well coincided with an earlier report [30]. Although Pex13 is a membrane-integral protein, since a large proportion of the C terminus of Pex13 protein is present outside of peroxisomes, and the anti-Pex13 antibodies used in this study were raised against the C terminus of Pex13 [29, 34], the band of Pex13 disappeared following treatment with proteinase K irrespective of the presence of Triton X-100 (Fig. 3D). Gpx1 was protected from proteinase K in the absence of Triton X-100. Taken together with the results of fractionation of peroxisomes (Fig. 3C), we concluded that Gpx1 is located in the peroxisomal matrix.

The peroxisomal matrix proteins contain a targeting signal that is sufficient to direct proteins into the peroxisomal lumen. The type 1 peroxisome targeting signal (PTS1; consensus sequence, S-K-L) has been found at the C terminus of many peroxisomal matrix proteins; while the type2 peroxisome targeting signal (PTS2) has been found only in a small number of enzymes, such as thiolase in *S. cerevisiae*. PTS2 (consensus sequence, R-L-X-X-X-X-H-L) occurs at the N terminus of peroxisomal proteins [35]. Pex5 and Pex7 are receptors for PTS1 and PTS2, respectively [35]. Meanwhile, some proteins containing no PTS have been reported to occur in peroxisomes. For example, Pox1, acyl-CoA oxidase, contains neither PTS1 nor PTS2; nevertheless, Pox1 is transported into the peroxisomal matrix in a Pex5-dependent manner [36]. On the other hand, Cta1 contains PTS1 at the C terminus, and consequently, Cta1 is present in peroxisomes [35]. Interestingly, the PTS1-deleted Cta1 (CTA1 Δ PTS1) is still able to be transported into the peroxisomal matrix [19], although the mechanism is unknown. Even though Gpx1 and Gpx3 are present in the peroxisomal matrix, they contain neither PTS1 nor

PTS2. Gpx1, and Gpx3 as well, might be transported into the peroxisomal matrix through binding to another protein that is transported into the peroxisomal matrix.

3.6. Peroxisomal Gpx1 shows peroxidase activity

We have demonstrated that Gpx1 is located in the peroxisomal matrix. Next, we examined whether the peroxisomal Gpx1 exhibits peroxidase activity. Since the amount of peroxisomes isolated by Nycodenz gradient ultracentrifugation was quite small, it was difficult to purify Gpx1 from peroxisomes. So, to evaluate the peroxidase activity of Gpx1 in the peroxisomal matrix, we determined the activity using the peroxisomal matrix fraction prepared from *gpx2Δgpx3Δ* and *gpx1Δgpx2Δgpx3Δ* cells. The subtraction of activities between these two strains is thought to correspond to Gpx1 activity. However, we suspected that a catalase may interfere with the evaluation of GPx peroxidase activity when H₂O₂ is used as a substrate. So, the peroxidase activity was measured under conditions in which the catalase activity was inhibited. Since Bayliak et al. [33] have reported that 90% of catalase activity was inhibited when yeast cells were incubated with 50 mM 3-amino 1,2,4-triazole (3-AT) for 5 h, we cultured cells in oleic acid medium for 20 h, and then added 50 mM 3-AT. After a 5-h incubation with 3-AT, cells were collected, and peroxisomes were purified. The peroxisomal matrix proteins were prepared, and incubated with 3-AT again for 5 h. We verified that catalase activity was greatly reduced compared with the peroxisomal matrix fraction prepared from cells that had not been treated with 3-AT (data not shown).

When H₂O₂ was used as a substrate, peroxidase activity was detected in the peroxisomal matrix fraction of *gpx2Δgpx3Δ* cells in both the glutathione system and thioredoxin system (Table 1); whereas, no activity was detected in the peroxisomal matrix fraction in *gpx1Δgpx2Δgpx3Δ* cells. Therefore, the peroxidase activity exhibited by the peroxisomal matrix fraction of *gpx2Δgpx3Δ* cells corresponds to that by peroxisomal Gpx1. On the other hand, when *t*-BHP was used as a substrate, no peroxidase activity was detected in the peroxisomal matrix fractions of *gpx2Δgpx3Δ* and *gpx1Δgpx2Δgpx3Δ* cells in the glutathione system. Whereas in the thioredoxin system, peroxidase activity was detected in the peroxisomal matrix of *gpx2Δgpx3Δ* and *gpx1Δgpx2Δgpx3Δ* cells (Table 1). The net activity of Gpx1 toward *t*-BHP would be obtained by the subtraction of these two values. We found that thioredoxin (Trx) and glutathione reductase (Glr1) were also present in peroxisomes in cells cultured in oleic acid medium (Fig. 3A). These results support our conclusion that Gpx1 functions as antioxidative enzyme in peroxisomes in the thioredoxin system and glutathione system, because

Trx serves as electron donor for peroxiredoxins and Glr1 is necessary for recycling of oxidized glutathione (glutathione disulfide) to reduced glutathione in coupling with the glutathione system.

Thioredoxin peroxidase activity toward *t*-BHP was detected even from the peroxisomes of *gpx1Δgpx2Δgpx3Δ*. Among thioredoxin peroxidases, Ahp1 has been reported to occur not only in the cytoplasm but also in peroxisomes [37]. We suspected that the thioredoxin peroxidase activity detected in the peroxisomal matrix of *gpx1Δgpx2Δgpx3Δ* cells might be due to Ahp1. Although almost all of Ahp1 protein was detected in the cytoplasm by Western blotting using anti-Ahp1 antibodies (data not shown), since Ahp1 is a homologue of alkyl hydroperoxide reductase, it may exhibit a higher specificity to *t*-BHP, an alkyl hydroperoxide.

3.7. Effect of GPX-deficiency on peroxisome biogenesis

To explore the role of Gpx1 in the growth in oleic acid medium, we focused on the biogenesis of peroxisomes. Peroxisomes were visualized using Pot1-GFP and DsRed-PTS1. The former contains PTS2 as a peroxisome-targeting sequence, and the latter contains PTS1. Fluorescence of GFP or DsRed, which represents the emergence of peroxisomes, was not observed in exponentially growing cells in glucose medium. At 24 h after the shift to oleic acid medium, punctate peroxisomes were observed in wild-type cells (Fig. 4A), and 50% of cells were found to contain the punctate peroxisomes (Fig. 4B). However, proportion of cells with peroxisomes was lower in cells defective in *GPXI* (*gpx1Δ*, *gpx1Δgpx3Δ*, *gpx1Δgpx2Δ*, and *gpx1Δgpx2Δgpx3Δ*) (Fig. 4B). Especially in *gpx1Δgpx2Δgpx3Δ* cells, the peroxisome formation was further impaired (Figs. 4A and 4B). To verify whether the deficiency in *GPXI* affects the peroxisome formation in oleic acid medium, *GPXI* was introduced into the *gpx1Δgpx2Δgpx3Δ* mutant with a low copy plasmid. As a result, the introduction of *GPXI* restored the peroxisome formation (Fig. 4A) as well as growth in oleic acid medium (Fig. 2B). Therefore, peroxisomal Gpx1 seems to influence the peroxisome formation in oleic acid medium. Essentially, the same results were obtained using DsRed-PTS1 in terms of the peroxisome formation in *gpx1Δgpx2Δgpx3Δ* cells in oleic acid medium (Supplementary Fig. S3).

3.8. GPX-deficiency does not affect the expression of peroxisomal proteins

It has been reported that fatty acid metabolism correlates with peroxisomal morphology, i.e. peroxisomal morphology was changed in a *pox1Δ* mutant defective in the initial step of β -oxidation [38]. To explore whether the expression of genes encoding

peroxisomal proteins involved in fatty acid metabolism was reduced in *gpx1Δgpx2Δgpx3Δ* cells thereby decreasing the formation of peroxisomes, the levels of Pot1, Cta1, and Pox1 proteins were determined. As shown in Figs. 5A and 5B, no distinct differences in the levels of these proteins were seen between the wild type and *gpx1Δgpx2Δgpx3Δ* mutant. We determined the peroxisomal distribution of Pot1 in *gpx1Δgpx2Δgpx3Δ* cells by Nycodenz gradient ultracentrifugation. The amount of Pot1 in peroxisomes was essentially the same between wild-type and *gpx1Δgpx2Δgpx3Δ* cells (Fig. 5C). In addition, the overexpression of *POX1* in *gpx1Δgpx2Δgpx3Δ* cells did not suppress the slow-growth phenotype and impairment of peroxisomal biogenesis in oleic acid medium (data not shown). Therefore, the expression of the genes encoding enzymes involved in the metabolism of oleic acid is not influenced by the deficiency in GPxs.

Considering the evidence in the literature, peroxisome biogenesis seems to be started by fusing pre-peroxisomal vesicles, generated from the ER, with pre-existing peroxisomes. Peroxisomal matrix proteins are then transported into the peroxisomes. Motley and Hettema [39] have reported that peroxisomes multiply through “growth and division”, and mature peroxisomes do not fuse. Peroxisome is divided by the actions of several proteins referred to as peroxins, such as Pex11, and the dynamin-related proteins Vps1 and Dnm1 [40]. Vps1 and Dnm1 are involved in the fission of peroxisomes [40]. Dnm1 was originally identified as a dynamin related-protein involved in mitochondrial fission [41], and Vps1 was identified as a protein required for vacuolar protein sorting and located in the Golgi apparatus [42]. Many peroxins, which are involved in the control of the assembly, size, and number of peroxisomes, have been identified in *S. cerevisiae* [40, 43, 44]. Pex11 was the first peroxin to be implicated in the division of peroxisomes [21, 40]. Pex25 and Pex27 were identified through sequence similarity with Pex11 [24, 40]. Pex28-29 and Pex30-32 were found, respectively, based on sequence similarity with Pex24 and Pex23 of *Yarrowia lipolytica* [45, 46]. Recently, Pex34 was reported as an interacting partner of Pex11 [47]. Pex11, Pex25, and Pex27 are located on the inner surface of the peroxisomal membrane [40, 44, 48]. Pex28, Pex29, Pex30, Pex31, Pex32, and Pex34 are peroxisomal membrane integral proteins, and involved in regulating peroxisomal size and number. Deficiency in these peroxins influences peroxisome biogenesis. To explore the effect of *GPX* deficiency on the expression of proteins involved in peroxisome biogenesis, we determined the levels of Pex11, Vps1, and Dnm1 in *gpx1Δgpx2Δgpx3Δ* cells cultured in oleic acid medium. As shown in Fig. 5D, no distinct differences in the levels of these proteins were observed between wild type and *gpx* null mutant. Additionally, we confirmed that Pex11 is

adequately distributed in peroxisomes in *gpx1Δgpx2Δgpx3Δ* cells (Fig. 5C). Therefore, a deficiency of GPxs is not likely to influence the levels of dynamin-related proteins and peroxins thereby affecting the formation of peroxisomes.

3.9. Role of Cys residues of Gpx1 in growth and peroxisome formation in oleic acid-containing medium

Previously, we have reported that Gpx1 is an atypical 2-Cys peroxiredoxin [12]. Since redox active coenzymes or prosthetic groups are not bound to atypical 2-Cys peroxiredoxins, an intramolecular disulfide bond is formed as a consequence of the peroxidase reaction [6]. In Gpx1, Cys³⁶ is the peroxidatic cysteine, which is attacked by peroxide to be oxidized to cysteine sulfenic acid (Cys-SOH). After which, Cys³⁶-SOH is reduced by other cysteines (Cys⁶⁴, Cys⁸², or Cys⁹⁶), referred to as resolving cysteine, in the same Gpx1 molecule, and consequently, an intramolecular disulfide bond is formed [12]. To explore whether redox regulation of Gpx1 is involved in the slow-growth phenotype of *gpx1Δgpx2Δgpx3Δ* cells in oleic acid medium, we introduced cysteine-substituted Gpx1 mutants into the *gpx* null mutant. The slow-growth phenotype of the *gpx1Δgpx2Δgpx3Δ* mutant was not complemented by the introduction of Gpx1^{C36S} (Fig. 6A). Resolving cysteine mutants (Gpx1^{C64S}, Gpx1^{C82S}, and Gpx1^{C96S}) moderately restored the growth in oleic acid medium. These results suggest that the redox regulation of Gpx1 is involved in the growth in oleic acid medium.

Next, we investigated the development of peroxisomes in *gpx1Δgpx2Δgpx3Δ* cells carrying Gpx1^{C36S}. As shown in Fig. 6B (also see Supplementary Fig. S4), proportion of cells with peroxisomes was reverted to those of wild-type cells when Gpx1^{WT} was introduced into *gpx1Δgpx2Δgpx3Δ* cells, although that in *gpx1Δgpx2Δgpx3Δ*+Gpx1^{C36S} cells was almost the same level as *gpx* null mutant carrying the vector alone. In *gpx1Δgpx2Δgpx3Δ* cells carrying resolving cysteine-substituted Gpx1 mutants (Gpx1^{C64S}, Gpx1^{C82S}, and Gpx1^{C96S}), proportion of cells with peroxisomes was increased after 24-48 h, although the levels were slightly lowered when compared with that of cells carrying Gpx1^{WT} (Fig. 6B). These results well coincided with the growth profiles of each cysteine-substituted Gpx1 mutant in oleic acid medium. Although Cys¹⁵² is not involved in redox regulation of Gpx1 [12], peroxisome formation in the *gpx* null mutant with Gpx1^{C152S} was delayed until 24 h after the shift to oleic acid medium; however, proportion of cells with peroxisomes was comparable with that with Gpx1^{WT} at 36-48 h (Fig. 6B). To verify whether Gpx1^{C36S} is adequately localized to peroxisomes, we performed Nycodenz gradient ultracentrifugation. As shown in Fig. 6C, Gpx1^{C36S} was located in

peroxisomes. These results suggest that the peroxidatic cysteine (Cys³⁶) of Gpx1 is involved in the growth and peroxisome formation in oleic acid medium, but not in the peroxisomal localization of Gpx1. To explore whether the roles of cysteine residues of Gpx1 are conserved in assimilating non-fermentable carbons in general, we determined the growth of *gpx1*Δ cells carrying each cysteine-substituted Gpx1 mutant in glycerol medium. However, substantially no differences in growth were seen among cysteine-substituted Gpx1 mutants (Supplementary Fig. S5), suggesting that Cys³⁶ of Gpx1 seems to play a role specifically in assimilating oleic acid as a carbon source. In addition, these results indicate that Gpx1^{C36S} does not affect the function of mitochondria, because integrity of mitochondria is necessary for assimilation of non-fermentable carbon in yeast.

Though we have no data that address the biochemical function of Gpx1 in terms of peroxisome biogenesis at present, we suspected that Gpx1 might influence peroxisome formation by interacting with peroxins *via* intermolecular disulfide bonds. For example, it has been reported that the activity of Pex11 is redox sensitive [48]. Although the biochemical properties of Pex11 remain to be determined, Marshall et al. [48] have reported that Pex11 is active when it is a monomer, and homodimerization occurs *via* the formation of an intermolecular disulfide bond between Cys³, which in turn limits the function of Pex11. So, we speculate that the peroxidatic cysteine of Gpx1 (Cys³⁶) protects Cys³ of Pex11 through the formation of an intermolecular mix-disulfide bond between Gpx1 and Pex11 to prevent the homodimerization of Pex11. If this is the case, homodimerization of Pex11 may occur easily in *gpx1*Δ*gpx2*Δ*gpx3*Δ cells. Subsequently, Pex11's function will be lost at an earlier stage of peroxisome biogenesis, which may lead to a delay in peroxisome formation thereby causing the slow-growth phenotype in oleic acid medium. A study to address the function of Gpx1 with respect to the redox status of Pex11 and formation of peroxisomes is now underway.

3.10. Conclusion

Among GPx homologues in *S. cerevisiae*, the expression of *GPXI* was induced when cells were cultured in oleic acid-containing medium. Gpx1 was present in the peroxisomal matrix, and peripheral of mitochondria. *gpx1*Δ cells showed slow-growth phenotype in oleic acid medium, which was due to the impairment of peroxisomal formation. The redox regulation of the peroxidatic Cys (Cys³⁶) of Gpx1 was involved in both peroxisome biogenesis and growth in oleic acid medium.

Acknowledgments

We thank Drs. V. C. Culotta, A. Hartig, W. H. Kunau, S. Kuge, J. M. Goodman, B. Distel, R. Erdmann, T. Endo, R. A. Rachubinski, and J. D. Aitchison for providing antibodies or plasmids. This research was partially supported by a Grant-in-Aid for Scientific Research from the Ministry of Education, Science, Sports and Culture of Japan.

References

- [1] R. J. A. Wanders, H. R. Waterham, *Biochemistry of mammalian peroxisomes revisited*, *Annu. Rev. Biochem.* 75 (2006) 295–332.
- [2] M. Kunze, I. Pracharoenwattana, S.M. Smith, A. Hartig, A central role for the peroxisomal membrane in glyoxylate cycle function, *Biochim. Biophys. Acta* 1763 (2006) 1441-1452.
- [3] Y. Poirier, V.D. Antonenkov, T. Glumoff, J.K. Hiltunen, Peroxisomal β -oxidation – a metabolic pathway with multiple functions, *Biochim. Biophys. Acta* 1763 (2006) 1413-1426.
- [4] L. A. Brown, A. Baker, Peroxisome biogenesis and the role of protein import, *J. Cell. Mol. Med.* 7 (2003) 388-400.
- [5] J. K. Hiltunen, A. M. Mursula, H. Rottensteiner, R. K. Wierenga, A. J. Kastaniotis, A. Gurvitz, The biochemistry of peroxisomal β -oxidation in the yeast *Saccharomyces cerevisiae*, *FEMS Microbiol. Rev.* 27 (2003) 35-64.
- [6] L. Flohé, H. Budde, B. Hofmann, Peroxiredoxins in antioxidant defense and redox regulation, *Biofactors* 19 (2003) 3-10.
- [7] S. G. Rhee, H. Z. Chae, K. Kim, Peroxiredoxins: a historical overview and speculative preview of novel mechanisms and emerging concepts in cell signaling, *Free Radic. Biol. Med.* 38 (2005) 1543-1552.
- [8] S. G. Park, M. K. Cha, W. Jeong, I. H. Kim, Distinct physiological functions of thiol peroxidase isoenzymes in *Saccharomyces cerevisiae*, *J. Biol. Chem.* 275 (2000) 5723-5732.
- [9] Y. Inoue, T. Matsuda, K. Sugiyama, S. Izawa, A. Kimura, Genetic analysis of glutathione peroxidase in oxidative stress response of *Saccharomyces cerevisiae*, *J. Biol. Chem.* 274 (1999) 27002-27009.
- [10] A. Delaunay, D. Pflieger, M. B. Barrault, J. Vinh, M. B. Toledano, A thiol peroxidase is an H₂O₂ receptor and redox-transducer in gene activation, *Cell* 111 (2002) 471–481.
- [11] T. Tanaka, S. Izawa, Y. Inoue, *GPX2*, encoding a phospholipid hydroperoxide glutathione

- peroxidase homologue, codes for an atypical 2-Cys peroxiredoxin in *Saccharomyces cerevisiae*, *J. Biol. Chem.* 280 (2005) 42078-42087.
- [12] T. Ohdate, K. Kita, Y. Inoue, Kinetics and redox regulation of Gpx1, an atypical 2-Cys peroxiredoxin, in *Saccharomyces cerevisiae*, *FEMS Yeast Res.* 10 (2010) 787-790.
- [13] Y. Ukai, T. Kishimoto, T. Ohdate, S. Izawa, Y. Inoue, Glutathione peroxidase 2 in *Saccharomyces cerevisiae* is distributed in mitochondria and involved in sporulation, *Biochem. Biophys. Res. Commun.* 411 (2011) 580-585.
- [14] Y. Inoue, Y. Tsujimoto, A. Kimura, Expression of the glyoxalase I gene of *Saccharomyces cerevisiae* is regulated by high osmolarity glycerol mitogen-activated protein kinase pathway in osmotic stress response, *J. Biol. Chem.* 273 (1998) 2977-2983.
- [15] F. J. Vizeacoumar, W. N. Vreden, M. Fagarasanu, G. A. Eitzen, J. D. Aitchison, R. A. Rachubinski, The dynamin-like protein Vps1p of the yeast *Saccharomyces cerevisiae* associates with peroxisomes in a Pex19p-dependent manner. *J. Biol. Chem.* 281 (2006) 12817-12823.
- [16] T. Ohdate, S. Izawa, K. Kita, Y. Inoue, Regulatory mechanism for expression of *GPXI* in response to glucose starvation and Ca^{2+} in *Saccharomyces cerevisiae*: Involvement of Snf1 and Ras/cAMP pathway in Ca^{2+} signaling, *Genes Cells* 15 (2010) 59-75.
- [17] K. Stade, C. S. Ford, C. Guthrie, K. Weis, Exportin 1 (Crm1p) is an essential nuclear export factor, *Cell* 90 (1997) 1041-1050.
- [18] R. Erdmann, W. H. Kunau, Purification and immunolocalization of the peroxisomal 3-oxoacyl-CoA thiolase from *Saccharomyces cerevisiae*, *Yeast* 10 (1994) 1173-1182.
- [19] F. Kragler, A. Langeder, J. Raupachova, M. Binder, A. Hartig, Two independent peroxisomal targeting signals in catalase A of *Saccharomyces cerevisiae*, *J. Cell Biol.* 120 (1993) 665-673.
- [20] S. Okazaki, T. Tachibana, A. Naganuma, N. Mano, S. Kuge, Multistep disulfide bond formation in Yap1 is required for sensing and transduction of H_2O_2 stress signal, *Mol. Cell* 27 (2007) 675-688.
- [21] P. A. Marshall, Y. I. Krimkevich, R. H. Lark, J. M. Dyer, M. Veenhuis, J. M. Goodman, Pmp27 promotes peroxisomal proliferation, *J. Cell Biol.* 129 (1995) 345-355.
- [22] K. Iwai, A. Naganuma, S. Kuge, Peroxiredoxin Ahp1 acts as a receptor for alkylhydroperoxides to induce disulfide bond formation in the Cad1 transcription factor, *J. Biol. Chem.* 285 (2010) 10598-10604.
- [23] N. H. Fukushima, E. Brisch, B. R. Keegan, W. Bleazard, J. M. Shaw, The GTPase effector

- domain sequence of the Dnm1p GTPase regulates self-assembly and controls a rate-limiting step in mitochondrial fission, *Mol. Biol. Cell* 12 (2001) 2756-2766.
- [24] J. J. Smith, M. Marelli, R. H. Christmas, F. J. Vizeacoumar, D. J. Dilworth, T. Ideker, T. Galitski, K. Dimitrov, R. A. Rachubinski, J. D. Aitchison, Transcriptome profiling to identify genes involved in peroxisome assembly and function, *J. Cell Biol.* 158 (2002) 259-271.
- [25] S. Izawa, K. Maeda, S. Sugiyama, J. Mano, Y. Inoue, A. Kimura, Thioredoxin deficiency causes the constitutive activation of Yap1, an AP-1-like transcription factor in *Saccharomyces cerevisiae*, *J. Biol. Chem.* 274 (1999) 28459–28465.
- [26] C. E. Outten, V. C. Culotta, Alternative start sites in the *Saccharomyces cerevisiae* *GLR1* gene are responsible for mitochondrial and cytosolic isoforms of glutathione reductase, *J. Biol. Chem.* 279 (2004) 7785-7791.
- [27] Y. Fujiki, A. L. Hubbard, S. Fowler, P. B. Lazarow, Isolation of intracellular membranes by means of sodium carbonate treatment: application to endoplasmic reticulum, *J. Cell Biol.* 93 (1982) 97–102.
- [28] F. Blobel, R. Erdmann, Identification of a yeast peroxisomal member of the family of AMP-binding proteins, *Eur. J. Biochem.* 240 (1996) 468-476.
- [29] Y. Elgersma, L. Kwast, A. Klein, T. Voorn-Brouwer, M. van den Berg, B. Metzger, T. America, H. F. Tabak, B. Distel, The SH3 domain of the *Saccharomyces cerevisiae* peroxisomal membrane protein Pex13p functions as a docking site for Pex5p, a mobile receptor for the import PTS1-containing proteins, *J. Cell Biol.* 135 (1996) 97-109.
- [30] J. Höhfeld, M. Veenhuis, W. H. Kunau, PAS3, a *Saccharomyces cerevisiae* gene encoding a peroxisomal integral membrane protein essential for peroxisome biogenesis, *J. Cell Biol.* 114 (1991) 1167-1178.
- [31] H. Yamamoto, M. Esaki, T. Kanamori, Y. Tamura, S. Nishikawa, T. Endo, Tim50 is a subunit of the TIM23 complex that links protein translocation across the outer and inner mitochondrial membranes, *Cell* 111 (2002) 519-528.
- [32] M. Naoe, Y. Ohwa, S. Ishikawa, C. Ohshima, S. Nishikawa, H. Yamamoto, T. Endo, Identification of Tim40 that mediates protein sorting to the mitochondrial intermembrane space, *J. Biol. Chem.* 279 (2004) 47815-47821.
- [33] M. Bayliak, D. Gospodaryov, H. Semchyshyn, V. Lushchak, Inhibition of catalase by aminotriazole in vivo results in reduction of glucose-6-phosphate dehydrogenase activity in *Saccharomyces cerevisiae* cells, *Biochemistry (Mosc.)* 73 (2008) 420-426.

- [34] S. J. Gould, J. E. Kalish, J. C. Morrell, J. Bjorkman, A. J. Urquhart, D. I. Crane, Pex13p is an SH3 protein of the peroxisome membrane and a docking factor for the predominantly cytoplasmic PTs1 receptor, *J. Cell. Biol.* 135 (1996) 85-95.
- [35] S. Subramani, Protein import into peroxisomes and biogenesis of the organelle, *Annu. Rev. Cell. Biol.* 9 (1993) 445-478.
- [36] A. T. Klein, M. van den Berg, G. Bottger, H. F. Tabak, B. Distel, *Saccharomyces cerevisiae* acyl-CoA oxidase follows a novel, non-PTS1, import pathway into peroxisomes that is dependent on Pex5p, *J. Biol. Chem.* 277 (2002) 25011-25019.
- [37] J. Lee, D. Spector, C. Godon, J. Labarre, M. B. Toledano, A new antioxidant with alkyl hydroperoxide defense properties in yeast, *J. Biol. Chem.* 274 (1999) 4537-4544.
- [38] C. W. van Roermund, H. F. Tabak, M. van Den Berg, R. J. Wanders, E. H. Hettema, Pex11p plays a primary role in medium-chain fatty acid oxidation, a process that affects peroxisome number and size in *Saccharomyces cerevisiae*, *J. Cell Biol.* 150 (2000) 489-498.
- [39] A. M. Motley, E. H. Hettema, Yeast peroxisomes multiply by growth and division, *J. Cell Biol.* 178 (2007) 399-3410.
- [40] Smith, J. J. and Aitchison, J. D. (2009) Regulation of peroxisome dynamics. *Curr. Opin. Cell Biol.* 21, 119-126
- [41] W. Bleazard, J. M. McCaffery, E. J. King, S. Bale, A. Mozdy, Q. Tieu, J. Nunnari, J. M. Shaw, The dynamin-related GTPase Dnm1 regulates mitochondrial fission in yeast, *Nat. Cell Biol.* 1 (1999) 298-304.
- [42] C. A. Vater, C. K. Raymond, K. Ekena, I. Howald-Stevenson, T. H. Stevens, The *VPS1* protein, a homolog of dynamin required for vacuolar protein sorting in *Saccharomyces cerevisiae*, is a GTPase with two functionally separable domains, *J. Cell Biol.* 119 (1992) 773-786.
- [43] P. B. Lazarow, Peroxisome biogenesis: advances and conundrums, *Curr. Opin. Cell Biol.* 15 (2003) 489-497.
- [44] M. Yan, N. Rayapuram, S. Subramani, The control of peroxisome number and size during division and proliferation, *Curr. Opin. Cell Biol.* 17 (2005) 376-383.
- [45] F. J. Vizeacoumar, J. C. Torres-Guzman, Y. Y. Tam, J. D. Aitchison, R. A. Rachubinski, *YHR150w* and *YDR479c* encode peroxisomal integral membrane proteins involved in the regulation of peroxisome number, size, and distribution in *Saccharomyces cerevisiae*, *J. Cell. Biol.* 161 (2003) 321-332.

- [46] F. J. Vizeacoumar, J. C. Torres-Guzman, D. Bouard, J. D. Aitchison, R. A. Rachubinski, Pex30p, Pex31p, and Pex32p form a family of peroxisomal integral membrane proteins regulating peroxisome size and number in *Saccharomyces cerevisiae*, *Mol. Biol. Cell* 15 (2004) 665-677.
- [47] R. J. Tower, A. Fagarasamu, J. D. Aitchison, R. A. Rachubinski, The peroxin Pex34p functions with the Pex11 family of peroxisomal divisional proteins to regulate the peroxisome population in yeast, *Mol. Biol. Cell* 22 (2011) 1727-1738.
- [48] P. A. Marshall, J. M. Dyer, M. E. Quick, J. M. Goodman, Redox-sensitive homodimerization of Pex11p: a proposed mechanism to regulate peroxisomal division, *J. Cell Biol.* 135 (1996) 123-137.

Figure legends

Fig. 1. Gpx1 expression was induced in medium containing oleic acid.

(A) Cells carrying *GPXI-3HA* at the *GPXI* locus were cultured in SD medium until a log phase of growth. After being transferred to YPOT medium, expression of each protein was determined at the prescribed time. To detect Gpx1, anti-HA monoclonal antibody was used. (B) *msn2Δmsn4Δ* cells carrying *GPXI-3HA* were cultured as described in (A), and the levels of each protein were determined.

Fig. 2. *gpx1Δ* cells showed slow growth in oleic acid-containing medium.

(A) Cells of each mutant were grown in SD medium until $A_{610}=1.0$. After being transferred to YNBOT medium, cell growth was monitored. (B) Cells of the wild type (WT) or *gpx1Δgpx2Δgpx3Δ* (*gpx1/2/3Δ*) mutant carrying pRS416 harboring *GPXI* (pRS416+GPX1) or *GPXI-3HA* (pRS416+GPX1-3HA) were cultured in SD medium until a log phase of growth, and transferred to YNBOT medium. The data shown are the average of 4 – 6 independent experiments. The standard error of the mean at each measuring point is within 5%.

Fig. 3. Localization of Gpx1.

(A) Wild-type cells were cultured for 20-24 h after being transferred from SD medium to YPOT medium, and homogenized as described in the Experimental. The P20 fraction was subjected to Nycodenz gradient ultracentrifugation to separate mitochondria (fraction nos. 1-3) and peroxisomes (fraction nos. 6-9). Pgk1 is a marker protein of the cytoplasm, and Por1 and Pot1 are markers of mitochondria and peroxisomes, respectively. (B) The purified mitochondrial pellets (C) were treated with 500 mM NaCl or 100 mM Na₂CO₃ in the presence of 0.6 M sorbitol. The mitochondrial pellets were then centrifuged, and resultant supernatants (S) and pellets (P) were subjected to SDS-PAGE followed by Western blotting. Hsp60 and Por1 are markers of the mitochondrial matrix and mitochondrial outer membrane, respectively. (C) The purified peroxisomes were fractionated as described in the Experimental. Lane 1, whole peroxisomes; lane 2, soluble fraction after hypoosmotic shock; lane 3, 1 M NaCl-extracted fraction; lane 4, high pH-extracted fraction; and lane 5, residual pellets after high pH-treatment. Pot1, peroxisomal matrix protein; Pcs60, membrane-associated protein; and Pex13, membrane-integral protein. (D) The purified peroxisomes from wild-type cells were treated with X-100, followed by 10 μg/ml proteinase K for the prescribed time.

Fig. 4. Effect of *GPX1* deficiency on peroxisome formation in oleic acid medium.

(A) Cells of the wild type (WT), *gpx1* Δ , or *gpx1* Δ *gpx2* Δ *gpx3* Δ mutants carrying Pot1-GFP were cultured in SD medium until a log phase of growth, collected by centrifugation, and transferred to YNBOT medium. Peroxisome formation in YNBOT medium was determined periodically by observation of Pot1-GFP using a fluorescence microscope. (B) Proportion of cells with peroxisomes was quantitated by counting the number of cells (200~300 cells in each experiment) showing fluorescence of Pot1-GFP at the prescribed time after transfer to oleic acid medium. Data are averages for three independent experiments \pm standard deviations.

Fig. 5. *GPX* deficiency does not affect the expression and targeting of peroxisomal proteins.

(A) Cells of the wild type (WT) or *gpx1* Δ *gpx2* Δ *gpx3* Δ (*gpx1/2/3* Δ) mutant were cultured in YNBOT medium, and the levels of Pot1 and Cta1 proteins were determined by Western blotting. (B) Cells of the wild type or *gpx1* Δ *gpx2* Δ *gpx3* Δ mutant carrying HA-Pox1 were cultured in YNBOT medium, and the level of Pox1 protein was determined by Western blotting using anti-HA monoclonal antibody. (C) Subcellular fractionation of the wild type or *gpx1* Δ *gpx2* Δ *gpx3* Δ cells was done as described in the legend of Fig. 3A. (D) Cells of the wild type and *gpx1* Δ *gpx2* Δ *gpx3* Δ mutant carrying *DNM1-HA* or *VPS1-GFP* were cultured in YNBOT medium.

Fig. 6. Role of Cys³⁶ of Gpx1 in growth and peroxisome formation in oleic acid medium.

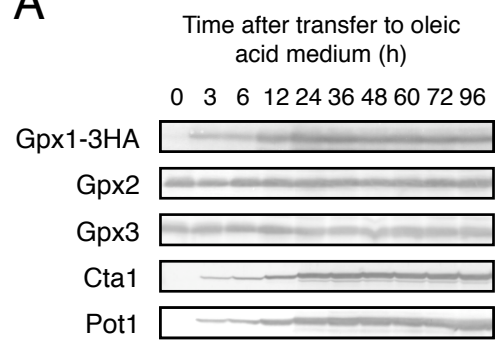
(A) Cells of the wild type (WT) or *gpx1* Δ *gpx2* Δ *gpx3* Δ (*gpx1/2/3* Δ) mutant carrying pRS416-based cysteine-to-serine substituted variants of Gpx1-3HA were cultured in SD medium until the $A_{610} = 1$, transferred to YNBOT medium, and cell growth was monitored. The data shown are the average of 4 – 6 independent experiments. The standard error of the mean at each measuring point is within 5%. (B) Cells of the wild type or *gpx1* Δ *gpx2* Δ *gpx3* Δ mutant carrying Pot1-GFP and pRS411-based cysteine-to-serine substituted variants of Gpx1-3HA were cultured in YNBOT medium, and peroxisome formation was determined periodically as described in the legend of Fig. 4B. Data are averages for three independent experiments \pm standard deviations. (C) *gpx1* Δ *gpx2* Δ *gpx3* Δ cells carrying pRS411-based Gpx1^{WT} (*left panel*) or Gpx1^{C36S} (*right panel*) were cultured in YNBOT medium, and subcellular fractionation was done as described in the legend of Fig. 3A.

Table 1

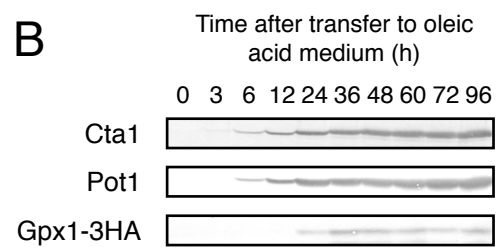
Peroxidase activity in peroxisomal matrix. GPx activity was measured with the glutathione (GSH) system (3 mM glutathione, 8.3 units/ml glutathione reductase, and 0.3 mM NADPH) and thioredoxin (TRX) system (4 μ M thioredoxin, 2 μ M thioredoxin reductase, and 0.3 mM NADPH) using 0.5 mM H₂O₂ or 0.5 mM *tert*-butyl hydroperoxide (*t*-BHP) as substrates [9]. N.D., not detected.

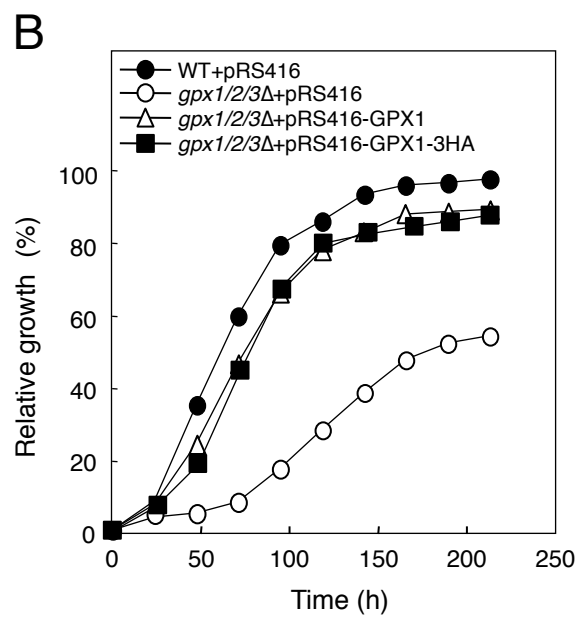
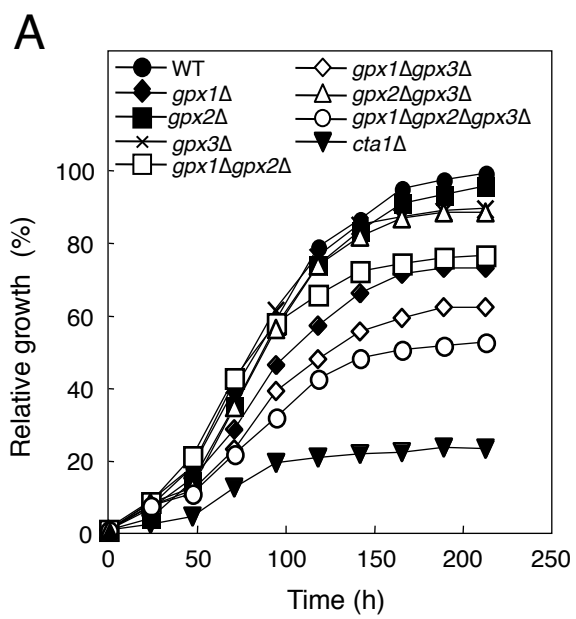
	GSH system (μ mol/min/mg protein)		TRX system (μ mol/min/mg protein)	
	<i>gpx2</i> Δ <i>gpx3</i> Δ	<i>gpx1</i> Δ <i>gpx2</i> Δ <i>gpx3</i> Δ	<i>gpx2</i> Δ <i>gpx3</i> Δ	<i>gpx1</i> Δ <i>gpx2</i> Δ <i>gpx3</i> Δ
H ₂ O ₂	0.120 \pm 0.059	N.D.	0.177 \pm 0.054	N.D.
<i>t</i> -BHP	N.D.	N.D.	0.531 \pm 0.068	0.177 \pm 0.068

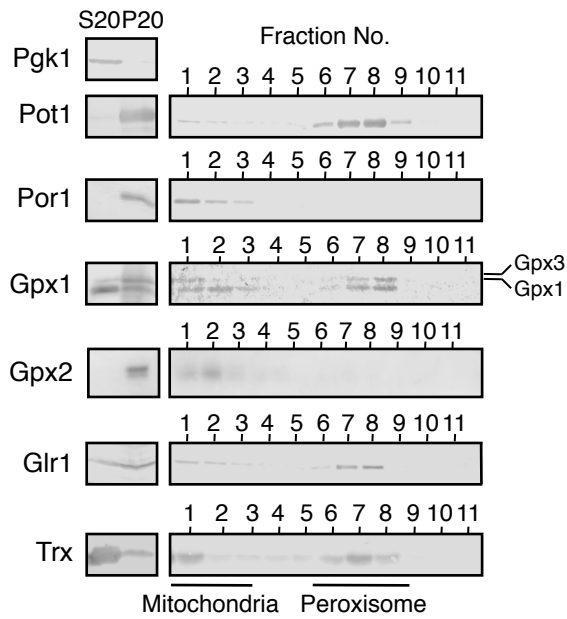
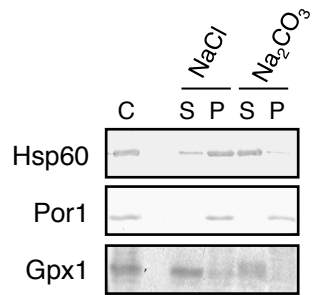
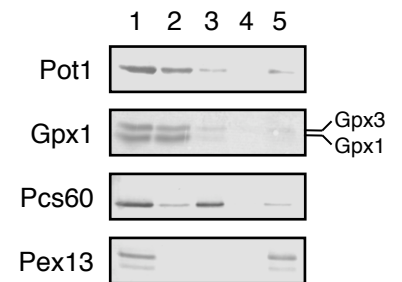
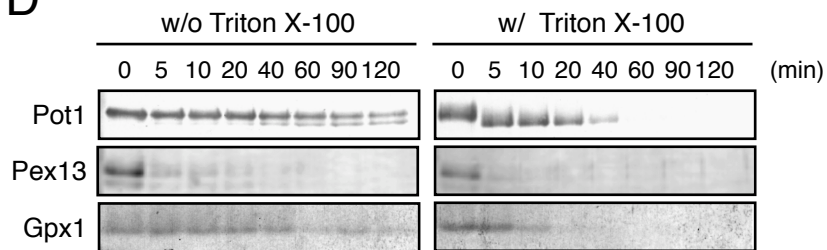
A



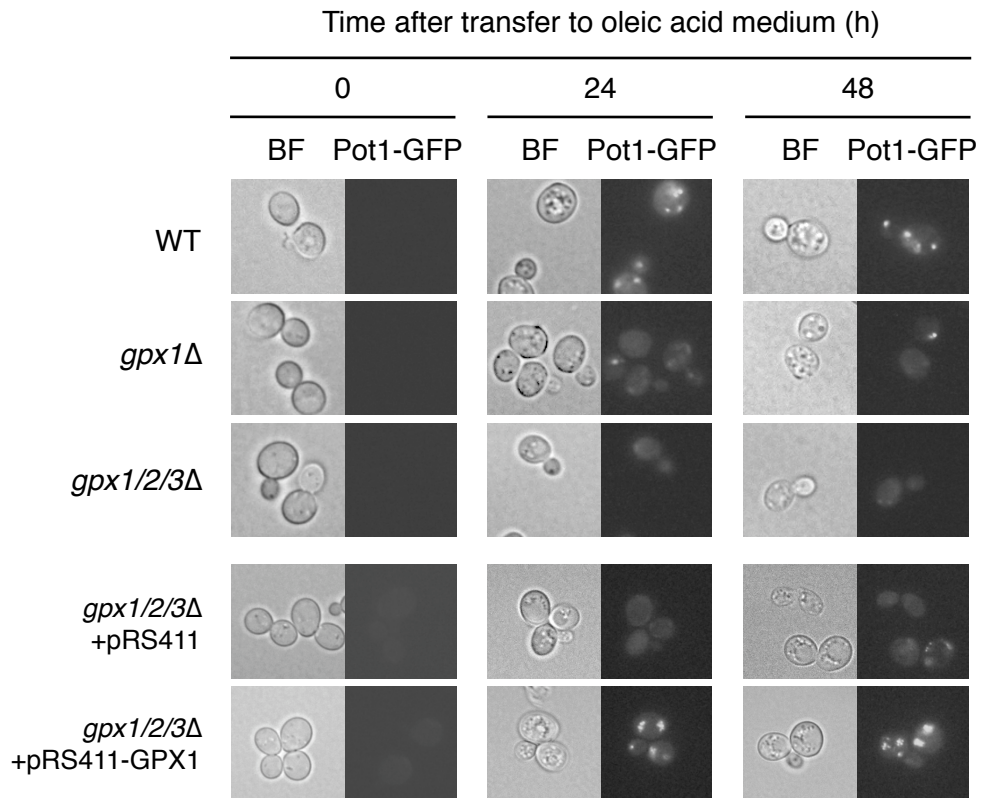
B



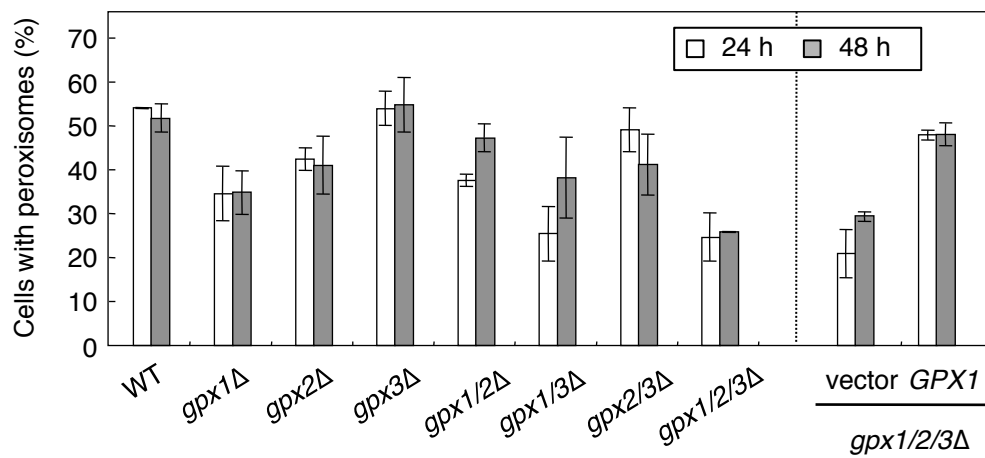


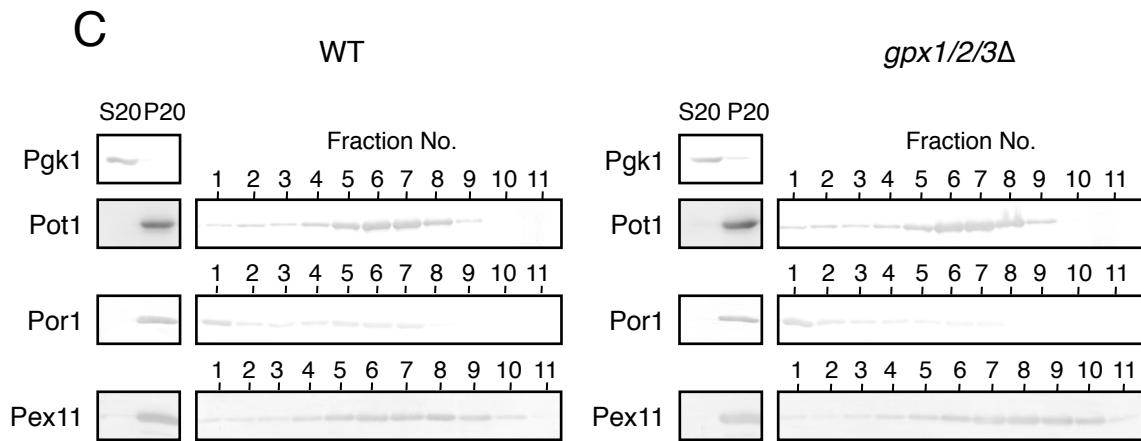
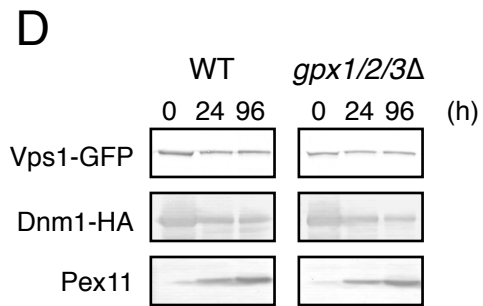
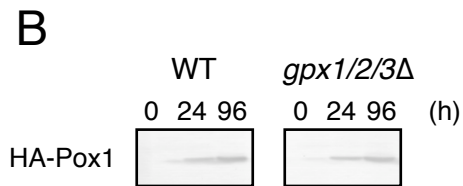
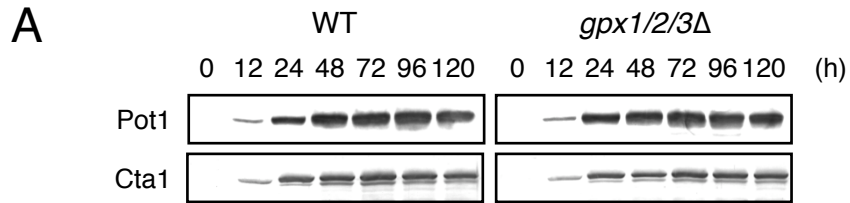
A**B****C****D**

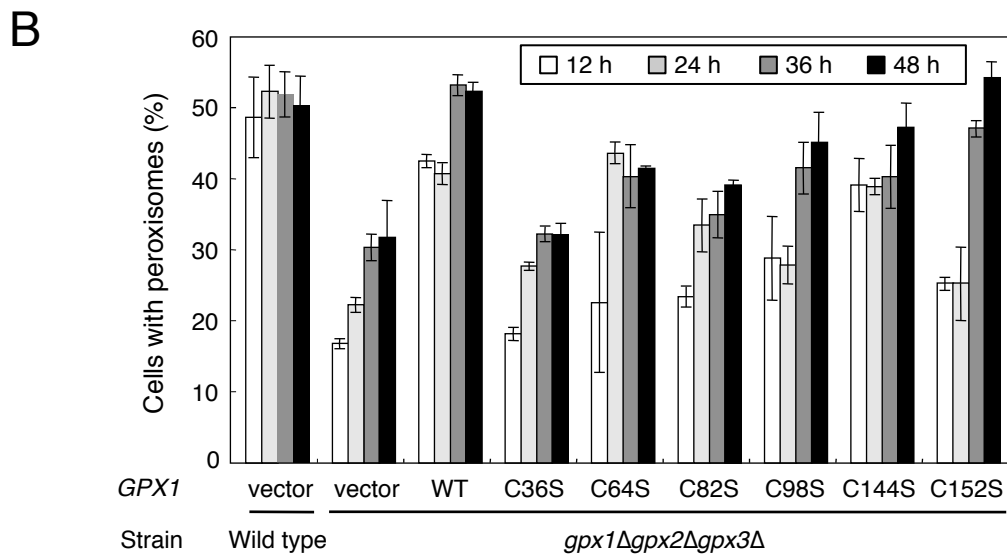
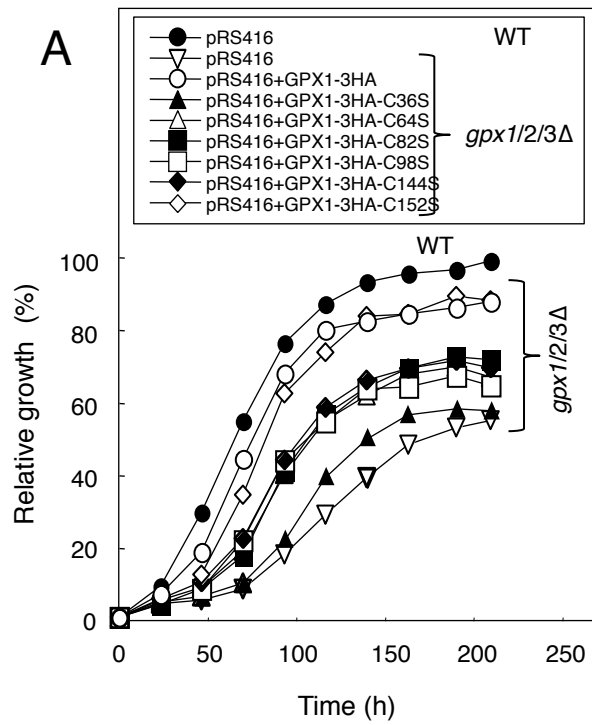
A



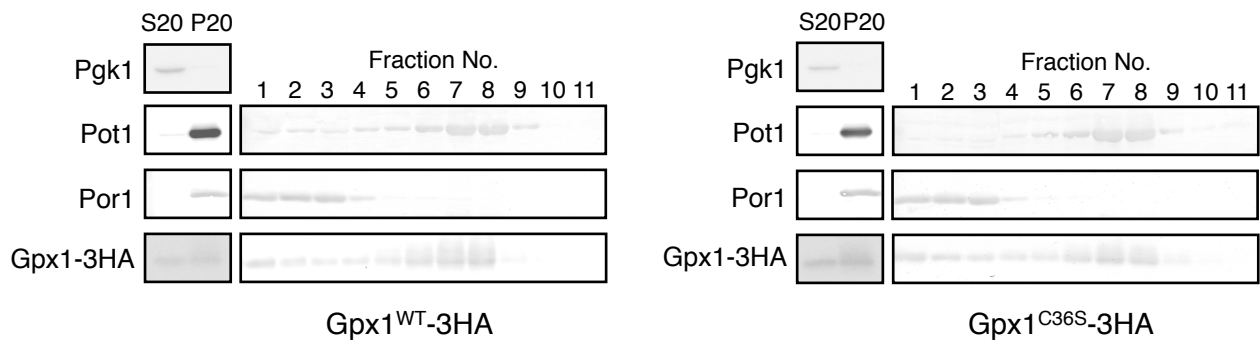
B







C



Supplementary Table S1

Strains used in this study

Strain	Relevant genotype	Source
BY4741 (WT)	<i>MATa his3 Δ 1 leu2 Δ 0 met15 Δ 0 ura3 Δ 0</i>	Euroscarf
<i>gpx1Δ</i>	BY4741, <i>gpx1Δ::his5⁺</i>	This study
<i>gpx2Δ</i>	BY4741, <i>gpx2Δ::kanMX4</i>	Euroscarf
<i>gpx3Δ</i>	BY4741, <i>gpx3Δ::LEU2</i>	This study
<i>gpx1Δgpx2Δ</i>	BY4741, <i>gpx1Δ::his5⁺ gpx2Δ::kanMX4</i>	This study
<i>gpx1Δgpx3Δ</i>	BY4741, <i>gpx1Δ::kanMX4, gpx3Δ::LEU2</i>	This study
<i>gpx2Δgpx3Δ</i>	BY4741, <i>gpx2Δ::kanMX4 gpx3Δ::LEU2</i>	This study
<i>gpx1Δgpx2Δgpx3Δ</i>	BY4741, <i>gpx1Δ:: his5⁺ gpx2Δ::kanMX4 gpx3Δ::LEU2</i>	This study
<i>cta1Δ</i>	BY4741, <i>cta1Δ::kanMX4</i>	Euroscarf
<i>msn2Δmsn4Δ</i>	BY4741, <i>msn2Δ::HIS3 msn4Δ::kanMX4</i>	This study
Pot1-GFP	BY4741, <i>POT1-GFP (URA3)</i>	This study
Vps1-GFP	BY4741, <i>VPS1-GFP (NAT)</i>	This study
HA-Pox1	BY4741, <i>HA-POX1 (URA3)</i>	This study

Supplementary Table S2

Primers used in this study

Name of primer	Sequence
GPX1-F	5'-ACCTTTCGATCCATCACCCAATAAA-3'
GPX1-R	5'-GGCTTTTCGGACTCATACCATATAG-3'
GPX1-F-XbaI	5'-ATACAAATCACATGGTCTAGAGATTGTGGC-3'
GPX1-R-BamHI	5'-TTCTCAAAGCGGATCCACTGAAAGGGTTCT-3'
GPX1-Sall-F	5'-GGAGTCGACGGACTTGATAGAATCCACCTT-3'
GPX1-PstI-R	5'-ACTATTCTGCAGGCTTTTCGGACTCATAAC-3'
GPX2-Sall-F	5'-AAGGAAAATACGGTCGACACTTACTAAATG-3'
GPX2-BamHI-R	5'-AATTCGGGAAAACGGATCCACTCATTAAAC-3'
GPX3-Sall-F	5'-CACTGCTTGATGTCGACTTCGGAGT-3'
GPX3-BamHI-R	5'-ACCATAACCTCAGAGGATCCGTATGCTGCT-3'
POT1-F	5'-TTTCTCAATGAGCTCATCGGGAGGTTTCCG-3'
POT1-R	5'-TTTAATAAGGATCCCGCGGCACCCATACC-3'
POX1-F-Sall	5'-AAGTGGTCACTCTCGAAAGTAGTCGACCTG-3'
POX1-HA-F	5'-CCCATACGATGTTCCAGATTACGCTACGAGACGTACTACTATTAATCCC-3'
POX1-HA-R	5'-CGTAATCTGGAACATCGTATGGGTACATATCGCAATACTAATTTATTAT-3'
POX1-R+900	5'-ATAACTACGTTTCTGAACTGGATCCAGCCA-3'
POX1-R-EagI	5'-AGAGAGGTATATAAAACACCGGCCGATTGG-3'
VPS1-GFP-F	5'-TGAACAACTTACATCAATACAGCCCATCC-3'
VPS1-GFP-R	5'-GGAAGCAGTTTACTCTCCTTCTATGTGTA-3'

Supplementary Table S3

Plasmids constructed in this study

Plasmid	Relevant description
pRS416+GPX1-3HA	pRS416 (<i>CEN</i> type, <i>URA3</i>), 3xHA tag is added at the C terminus of Gpx1
pRS306+GPX1-3HA	pRS306 (integrate-type, <i>URA3</i>), <i>GPX1-3HA</i> is integrated into the <i>GPX1</i> locus after digestion with EcoRI
pRS414+GPX1	pRS414 (<i>CEN</i> type, <i>LEU2</i>) harboring <i>GPX1</i> with own promoter
pRS411+GPX1	pRS411 (<i>CEN</i> type, <i>MET15</i>) harboring <i>GPX1</i> with own promoter
pRS416+GPX1	Harboring <i>GPX1</i> with own promoter
pRS426+GPX1	pRS426 (2 μ , <i>URA3</i>), carrying <i>GPX1</i> with own promoter
pRS416+GPX2	Harboring <i>GPX2</i> with own promoter
pRS416+GPX3	Harboring <i>GPX3</i> with own promoter
pRS411+GPX2	Harboring <i>GPX2</i> with own promoter
pRS411+GPX3	Harboring <i>GPX3</i> with own promoter
pRS411+Gpx1 ^{WT}	Harboring <i>GPX1-HA</i> with own promoter
pRS411+Gpx1 ^{C36S}	Harboring Cys ³⁶ to Ser mutant of <i>GPX1-3HA</i> with own promoter
pRS411+Gpx1 ^{C64S}	Harboring Cys ⁶⁴ to Ser mutant of <i>GPX1-3HA</i> with own promoter
pRS411+Gpx1 ^{C82S}	Harboring Cys ⁸² to Ser mutant of <i>GPX1-3HA</i> with own promoter
pRS411+Gpx1 ^{C98S}	Harboring Cys ⁹⁸ to Ser mutant of <i>GPX1-3HA</i> with own promoter
pRS411+Gpx1 ^{C144S}	Harboring Cys ¹⁴⁴ to Ser mutant of <i>GPX1-3HA</i> with own promoter
pRS411+Gpx1 ^{C152S}	Harboring Cys ¹⁵² to Ser mutant of <i>GPX1-3HA</i> with own promoter
pRS411+GPX1-PTS1	PTS1 is added at the C terminus of Gpx1
pRS416+GPX1-PTS1	PTS1 is added at the C terminus of Gpx1
pRS306+POT1-GFP	<i>POT1-GFP</i> is integrated into the <i>POT1</i> locus after digestion with EcoRI
pRS306+HA-POX1	HA-tag is added at the N terminus of <i>POX1</i> , and <i>HA-POX1</i> is integrated at the <i>POX1</i> locus after digestion with HindIII
pRS421+POX1	pRS421 (2 μ , <i>MET15</i>) harboring <i>POX1</i> with own promoter

Legends for Supplementary figures

Supplementary Figure S1. Validation of anti-Gpx1 antibodies.

Cells of each *gpx* mutant in BY4741 background (*gpx1* Δ , *gpx1* Δ ::*KanMX4*; *gpx2* Δ , *gpx2* Δ ::*KanMX4*; *gpx3* Δ , *gpx3* Δ ::*LEU2*; *gpx1* Δ *gpx2* Δ , *gpx1* Δ ::*his5*⁺ *gpx2* Δ ::*KanMX4*; *gpx1* Δ *gpx3* Δ , *gpx1* Δ ::*KanMX4* *gpx3* Δ ::*LEU2*; *gpx2* Δ *gpx3* Δ , *gpx2* Δ ::*KanMX4* *gpx3* Δ ::*LEU2*, *gpx1* Δ *gpx2* Δ *gpx3* Δ , *gpx1* Δ ::*his5*⁺ *gpx2* Δ ::*KanMX4* *gpx3* Δ ::*LEU2*) were cultured in YPD medium for 2 days, and cell extracts were prepared. After separation of each cell extract by SDS-SAGE, Western blotting was conducted using anti-Gpx1 antibodies. Anti-Gpx1 antibodies raised crossed with Gpx3 also.

Supplementary Figure S2. Localization of Gpx1.

(A) *gpx1* Δ cells carrying Gpx1-3HA were cultured in YNBOT medium, and localization of Gpx1-3HA was determined by indirect immunofluorescence microscopy using anti-HA monoclonal antibody. The cells were stained for DNA with 1 μ g/ml 4',6'-diamino-2-phenylindole dihydrochloride (DAPI). (B) *gpx1* Δ cells were cultured for 20-24 h after being transferred from SD medium to YPOT medium, and homogenized as described in the Experimental. The P20 fraction was subjected to Nycodenz gradient ultracentrifugation to separate mitochondria and peroxisomes. Pgk1 is a marker protein of the cytoplasm, and Por1 and Pot1 are markers of mitochondria and peroxisomes, respectively. Gpx1-3HA and Gpx3 were detected using anti-HA monoclonal antibody and anti-Gpx3 antibodies, respectively.

Supplementary Figure S3. Effect of GPX deficiency on peroxisome formation.

Cells of wild type (WT) or *gpx1* Δ *gpx2* Δ *gpx3* Δ mutant carrying DsRed-PTS1 were cultured as described in SD medium until the log phase of growth, transferred to YNBOT medium, and peroxisome formation was determined periodically.

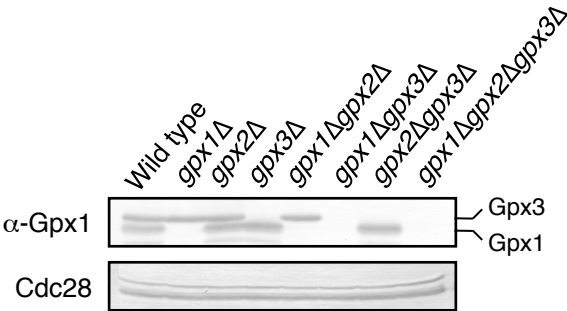
Supplementary Figure S4. Role of Cys³⁶ of Gpx1 in peroxisome formation in oleic acid medium.

Cells of the wild type (WT) or *gpx1* Δ *gpx2* Δ *gpx3* Δ (*gpx1/2/3* Δ) mutant carrying Pot1-GFP and the *CEN*-type plasmid pRS411-based cysteine-to-serine substituted variants of Gpx1-HA were cultured in YNBOT medium, and peroxisome formation was determined periodically.

Supplementary Figure S5. Growth of *gpx1* Δ cells carrying various Cys-substituted Gpx1 mutants in glycerol medium.

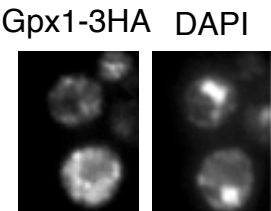
Cells of the wild type (WT) or *gpx1* Δ *gpx2* Δ *gpx3* Δ (*gpx1/2/3* Δ) mutant carrying pRS416-based cysteine-to-serine substituted variants of Gpx1-3HA were cultured in SD medium until the $A_{610} = 1$, transferred to glycerol medium (2% glycerol, 0.67% yeast nitrogen base without amino acids) supplemented with appropriate amino acids and bases, and cell growth was monitored. The data shown are the average of three independent experiments. The standard error of the mean at each measuring point is within 5%.

Supplementary Fig. S1



Supplementary Fig. S2

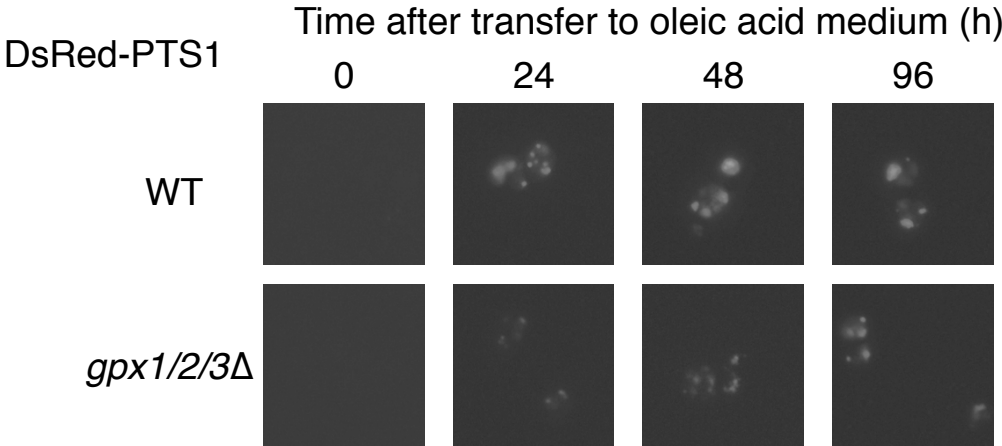
A



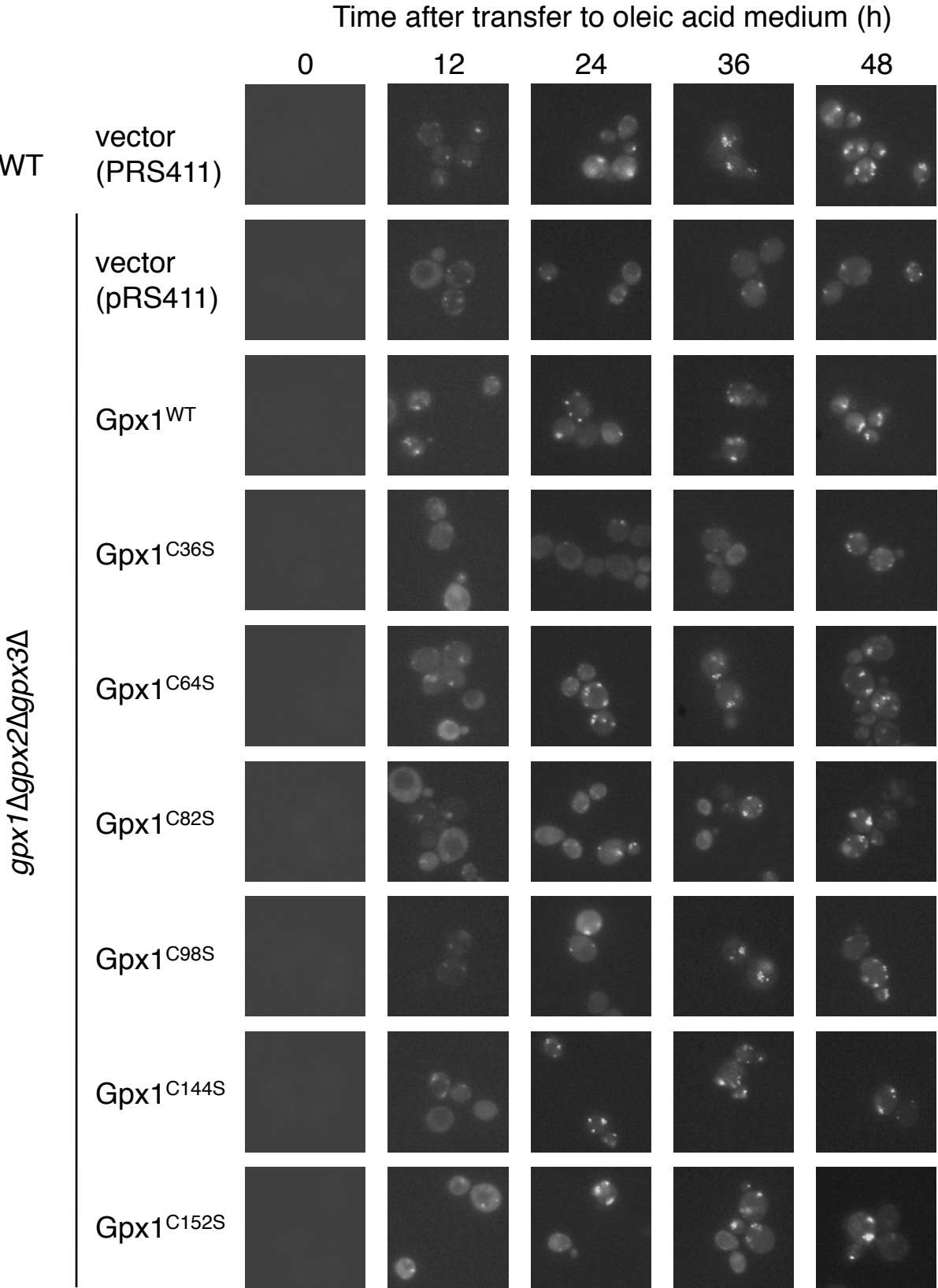
B



Supplementary Fig. S3



Supplementary Fig. S4



Supplementary Fig. S5

